Journal of Applied Polymer Science

PMMA/o-MMT Nanocomposites Obtained Using Thermally Stable Surfactants

Giovanna Di Pasquale, Antonino Pollicino
Department of Industrial Engineering, University of Catania, Catania, Italia
Correspondence to: A. Pollicino (E-mail: apollicino@dii.unict.it)

ABSTRACT: In the preparation of polymer/montmorillonite (MMT) nanocomposites, the commonly used compatibilizers (cations of long carbon-chain alkyl ammonium salts) present the drawback of a poor thermal stability. During bulk processing of nanocomposites elevated temperatures are usually required and, if processing temperature is close to decomposition temperature of the surfactant, decomposition will occur altering the interface between filler and polymer. To solve this problem, organically modified MMTs with thermally stable imidazolium surfactants have been prepared. A series of nanocomposites were obtained by dispersing o-MMT in poly(methyl methacryate) (PMMA) matrix via an *in situ* free radical polymerization. The nanocomposites were characterized by X-ray diffraction, transmission electron microscopy, gel permeation chromatography, thermogravimetric analysis, dynamic mechanical analysis, and nanoindentation measurements. The results showed that nanocomposite thermal stability depended on both the kind of used surfactant and degree of exfoliation. Under the same values of molecular weight, the nanocomposites containing imidazolium cations showed a better thermal stability with respect to the nanocomposite obtained using a standard alkylammonium surfactant. Dynamic mechanical and Nanoindentation measurements showed an improvement of mechanical properties, such as modulus and hardness, with respect to pure PMMA. Solution blending treatments on these nanocomposites led to obtaining of further improvement of the thermal performance. © 2014 Wiley Periodicals, Inc. J. Appl. Polym. Sci. **2015**, *132*, 41393.

KEYWORDS: clay; nanostructured polymers; structure-property relations; surfactants; thermogravimetric analysis (TGA)

Received 17 March 2014; accepted 11 August 2014
DOI: 10.1002/app.41393

INTRODUCTION

During last decades, much researcher attention has been directed to the study of polymer/phyllosilicate nanocomposites. In these materials, the nanometric dispersion of low amounts of silicate determines interesting enhancements of mechanical, thermal, and flame retardation properties. Such enhancements depend on the dimension and on the degree of dispersion (exfoliation) of silicate layers.[1–6]

The clay platelet nanometric dispersion into the polymeric matrix reduces the mobility of the macromolecular chains inducing an appreciable reinforcing effect, while the high interface area makes possible an efficient stress transfer from the matrix to the filler with the consequence of enhancement of mechanical properties such as Young's modulus and toughness. Besides to these beneficial effects a drawback emerged regarding the UV photostability of these nanocomposites, and we have demonstrated that the degree of exfoliation negatively affects the UV photostability of polymer/clay nanocomposites.[7]

One of the most used phyllosilicates in nanocomposites is montmorillonite (MMT). Each MMT layer is 1 nm thick while lateral dimensions can vary from 300 Å to several microns. The polymer/MMT nanocomposites may show an intercalated structure in which MMT layers are well ordered and polymer chains are inserted into the gallery space of the silicate.[8,9]

When individual silicate layers are no longer close enough and are homogeneously distributed in the polymer matrix there is an exfoliated (or delaminated) structure. Exfoliation ensures the higher nanocomposite performances.

During preparation of this kind of nanocomposites, the MMT organic modification is a crucial step. In fact, interactions between polymer matrix and clay platelets determine the possibility of obtaining exfoliation. For this reason, the first step is to modify the platelet surface using cationic surfactants able to enlarge the distance among MMT layers ensuring a good interfacial interaction with polymer matrix. Moreover, because high temperature is reached during processing, the thermal stability of the organic surfactants plays an important role. It is well know that commonly used organomodification agents (long carbon chain alkyl ammonium salts) undergo to Hoffman degradation[10] in the range of 150–300°C, and show a poor thermal stability.

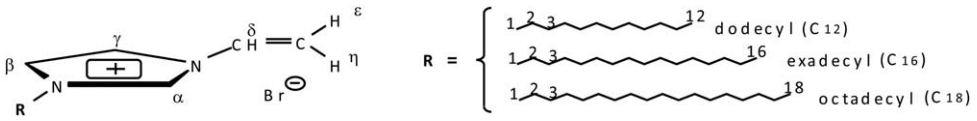

Scheme 1. Structure of C_{12}, C_{16}, and C_{18} cations used to organic modification of MMT.

Imidazolium cations, because of charge delocalization, present a higher thermal stability, and then can promote a higher thermal stability of the whole nanocomposite. In the literature, there are a large number of studies on the modification of MMT with imidazole surfactants and their use for the preparation of polymer nanocomposites.[11–23] The use of these surfactants allows to significantly improve the thermal stability of the organically modified clay thus allowing the possibility of achieving higher process temperatures.

In last years, there has been interest on poly(methyl methacrylate) (PMMA)/clay nanocomposites and many papers have appeared in the literature most of which try to study how to improve the performance of the systems.[22,24–33]

Despite the high number of studies on these topics, to the best of our knowledge, only recently a study has been presented on the preparation of PMMA clay nanocomposites in which the organic modification of the clay was carried out using an imidazolium surfactant.[22] In this study, the used modifier is an imidazolium cation having in its structure an alkyl chain of 12 carbon atoms (1-dodecyl-3-methylimidazolium hexafluorophosphate). It is known that the length of the alkyl chain affects the degree of clay exfoliation in the nanocomposite and then we decided to study the effect of using MMT organically modified with imidazolium cations having longer alkyl chains (C16 and C18) with the purpose of obtaining an improvement of the thermal and mechanical performance of PMMA. In this article, we describe the preparation and the characterization of a series of PMMA/o-MMT nanocomposite where the o-MMTs were prepared via ion exchange reaction using thermally stable functionalized imidazolium salts (C_{12}, C_{16}, and C_{18}—Scheme 1) that have in their structure a vinyl group. Such functionalization can promote delamination.[34,35]

The PMMA/o-MMT nanocomposites were obtained via *in situ* free radical polymerization of methyl methacrylate (MMA) monomer in the presence of organomodified MMTs (C_{12}, C_{16}, and C_{18}/MMT) and 2,2′-azobis(isobutyrronitrile) (AIBN) as initiator. In the second stage, some of the obtained nanocomposites have been solubilized in tetrahydrofuran (THF) and precipitated in water. The aim of this treatment has been to obtain a higher degree of exfoliation exploiting the fact that solvent molecules, because of the organophilic nature of the surfactants, inserting among the gallery spacings disrupt the registry between the clay layers. The nanocomposites were characterized by X-ray diffraction (XRD), transmission electron microscopy (TEM), gel permeation chromatography (GPC), thermogravimetric analysis (TGA), dynamic mechanical analysis (DMA), and nanoindentation measurements.

EXPERIMENTAL

Materials

The chemicals used in this study were acquired from Aldrich Chemical. The MMT (Na/MMT) is a fine powder with a particle size of 10–15 μm in a dry state and a cation exchange capacity of 100 mEq/100 g. MMA monomer was purified using an inhibitor removal column, also acquired from Aldrich. AIBN was purified by crystallizing twice from dry ethanol at temperature less than 40°C and out of direct light.

Instruments

Thermal degradations were performed in a Mettler TA 3000 thermogravimetric analyser coupled with a Mettler TC 10A processor. Degradations were performed in the scanning mode, from 30°C up to 900°C, in both flowing nitrogen (0.02 L/min) and in static air atmosphere, at heating rate of 10°C/min.

The molecular weight results were determined using an HP 1100 GPC instrument, equipped with a refractive index detector, operating at 30°C, using THF as carrier at a flow rate of 1 mL min^{-1}. Separations were accomplished using a PLgel 5 μm mixed-D column connected with a PL gel 5 μm 500 Å column (Polymer Labs). The measurement utilized a refractive index detector and toluene as internal standard. Solution concentrations were 2 mg/mL in THF; they were filtered through 0.45 μm PTFE membranes and injected into the columns in 20 μm aliquots. Calibration was performed using narrow polydispersity polystyrene standards in weight average molecular weights in the range 2500–400,000 Da.

XRD measurements were recorded on a Bruker-AXS D5005 $\theta-\theta$ X-ray diffractometer, using Cu K_α radiation operating at 20 kV and 30 mA.

Sample for TEM analysis were prepared using an ultramicrotome and placed on a 100 mesh copper grid for analysis. The TEM investigation was performed on a Jeol JEM 2010 operating at an acceleration voltage of 200 kV.

Films of the samples with a thickness of 100 μm were obtained by means of a Gradeby Specac P/N15800 press, heating the material, reduced to powder, at 170°C for 2 min and then applying a force of 2 tons per another 2 min.

DMA was conducted, using a DMA TRITEC 2000, using a tensile configuration on the test specimens (films with thickness of about 100 μm). The tests were performed by applying a 10 Hz frequency, in a temperature range from 25 to 145°C with a heating rate of 5°C/min and with an amplitude of the stress of 0.01%.

Nanoindentation measurements (Nano Hardness Tester, CSM Instruments SA) have been performed with a diamond Berkovich indenter. For the evaluation of the load/displacement curves, the method of Oliver and Pharr has been used at a penetration depth of 0.5 μm, thereby assuming a Poisson's ratio of 0.3. For each sample, a number of indentations have been performed at different positions; if not indicated otherwise, the results given below are the averages.

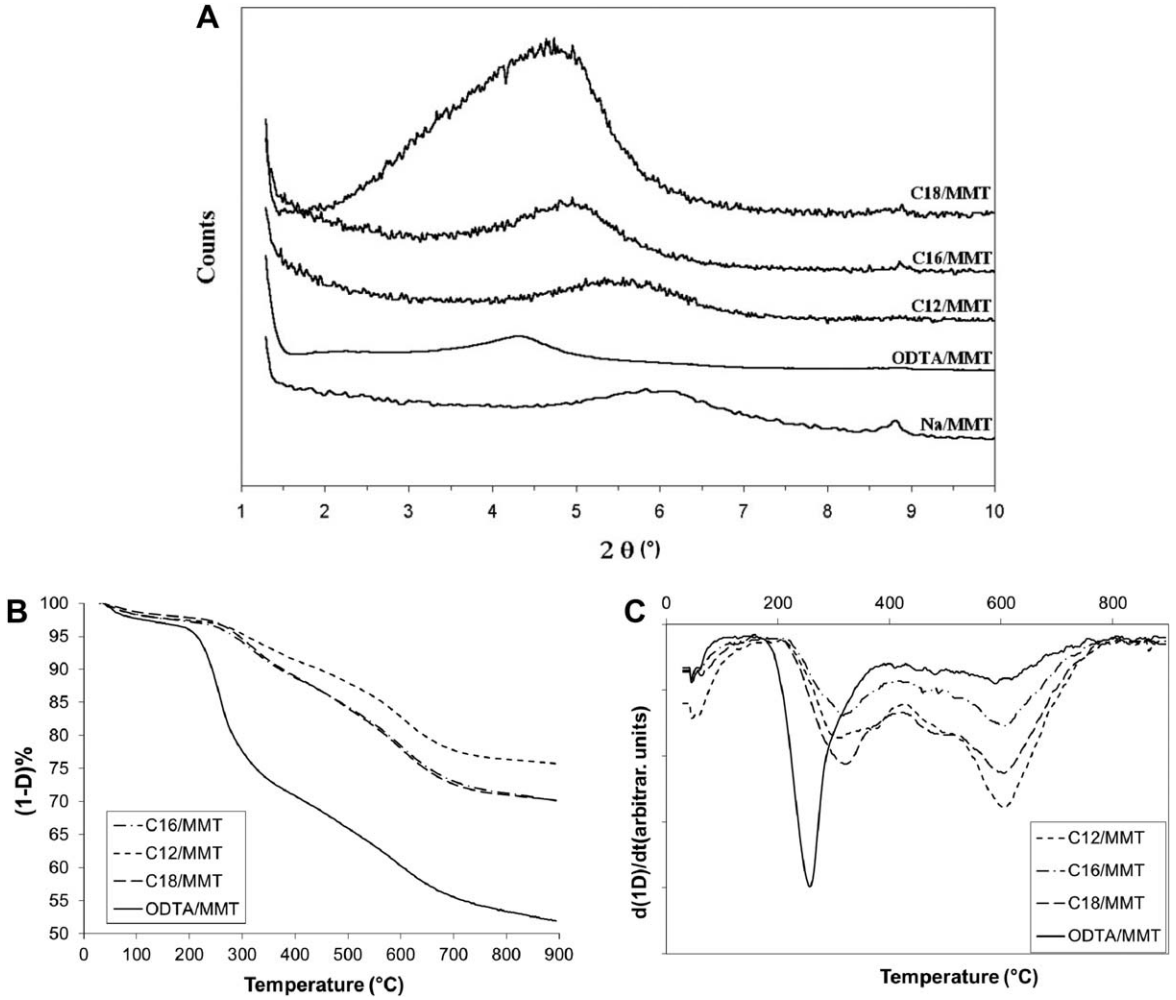

Figure 1. (A) XRD patterns of pristine and o-MMTs; TGA (B) and DTGA (C) curves under static air atmosphere of ODTA/MMT, C_{18}/MMT, C_{16}/MMT, and C_{12}/MMT.

Synthesis of Imidazolium Salts

The synthesis and the characterization of the imidazolium salts are described in our previous work.[13]

Preparation of o-MMT

An aqueous suspension of 2.088 g of prewashed Na/MMT in 200.0 mL of deionized water was added to a solution obtained dissolving 2.506 mmol of imidazolium salt in 10.00 mL of a 50 : 50 mixture of ethanol and deionized H_2O at 50°C. After the solution was stirred in inert atmosphere for 6 h at 50°C, the white powder was filtered, washed several times with a mixture of ethanol, and deionized water until no bromide ion could be detected by an $AgNO_3$ aqueous solution, and then dried in a vacuum oven overnight at room temperature.

The organomodification of clay with octadecyltrimethylammonium bromide (ODTA) was carried out using the same procedure described above with the exception of the solvent. In this case, deionized H_2O was used.

Preparation of PMMA/o-MMT Nanocomposites by Bulk Polymerization (BP)

As a typical procedure for the preparation PMMA materials via *in situ* free radical polymerization, an appropriate amount of organophilic clay, calculated by 3 wt % (0.3600 g) with respect to MMA was thoroughly dispersed in 12.00 g of MMA monomer. First, the suspension was stirred at room temperature under flowing N_2 gas until it became homogeneous (7 h), then it was sonicated for 1 h; finally 0.0600 g (0.5 wt %) of AIBN initiator was added to monomer clay mixture. The tube was degassed by three freeze-thaw cycles, sealed at 0.01 mmHg, and placed in a constant temperature bath at 60°C for 16 h to obtain PMMA/clay nanocomposites. A bulk polymerization of PMMA was carried out at the same condition used for the nanocomposites except for the absence of the clay.

The samples used for GPC measurements were obtained as follows: the nanocomposites were extracted using toluene at room temperature and repeatedly filtered, to ensure the removal of the clay. The PMMAs obtained by precipitation in methanol were used to prepare the solutions.

Preparation of PMMA/o-MMT Nanocomposites by Solution Blending (SB)

Nanocomposites obtained by *in situ* polymerization have been solubilized in THF, precipitated in water, washed with petroleum ether, and left in vacuum oven for 12 h at 40°C.

Table I. Interlayer d° Spacings, Decomposition Temperature at 5 and 10% Weight Loss (T_{d5} and T_{d10}), Molecular Weights, and Polydispersion Coefficient of Pristine MMT, o-MMTs, and their Nanocomposites

Sample	d° (nm)	T_{d5} (°C)[a]	T_{d10} (°C)[a]	M_n (x10^{-4})	M_w (x10^{-4})	$d_c = M_w/M_n$
MMT	1.48	353	607	-	-	-
ODTA/MMT	2.05	251	272	-	-	-
C_{12}/MMT	1.61	423	564	-	-	-
C_{16}/MMT	1.80	370	501	-	-	-
C_{18}/MMT	1.88	354	474	-	-	-
PMMA BP	-	255	274	39.60	48.24	1.22
PMMA/MMT BP	1.67	250	274	39.97	49.64	1.24
PMMA/MMT/ODTA BP	4.01	257	292	44.86	54.16	1.21
PMMA/C_{12}/MMT BP	3.68	249	291	26.14	33.38	1.28
PMMA/C_{16}/MMT BP	3.18	251	291	31.58	39.50	1.25
PMMA/C_{18}/MMT BP	4.10	299	319	41.13	50.69	1.23
PMMA/MMT/ODTA SB	-	287	307	44.86	54.16	1.21
PMMA/C_{12}/MMT SB	-	291	308	26.14	33.38	1.28
PMMA/C_{16}/MMT SB	-	292	312	31.58	39.50	1.25
PMMA/C_{18}/MMT SB	-	297	321	40.80	51.98	1.27

[a] Determined in nitrogen.

RESULTS AND DISCUSSION

The crystal structure of MMT consists of two-dimensional layers with adsorbed exchangeable alkali or alkaline earth cations. The layers are formed by fusing two silica tetrahedral sheets to an edge-shared octahedral sheet of aluminum hydroxide. During the cationic exchange process, the organic cations (ODTA, C_{12}, C_{16}, and C_{18}) penetrated the interlayer space, replacing the alkaline cations. The interlayer d° spacings were determined by wide-angle powder XRD and calculated from Bragg's law: $d^{\circ} = \lambda/(2\sin\theta)$ at peak position. All of the o-MMT had larger d°-spacings than pristine MMT due to the larger volume of organic cations. In fact, after the organic cations intercalated into the galleries, the d° spacings showed an increase from 1.48 nm in MMT to 1.61, 1.80, and 1.88 nm in C_{12}, C_{16}, and C_{18}/MMT, respectively [Figure 1(A), Table I]. As expected, d° increased with alkyl chain length. A higher d° (2.05 nm) was showed by ODTA/MMT.

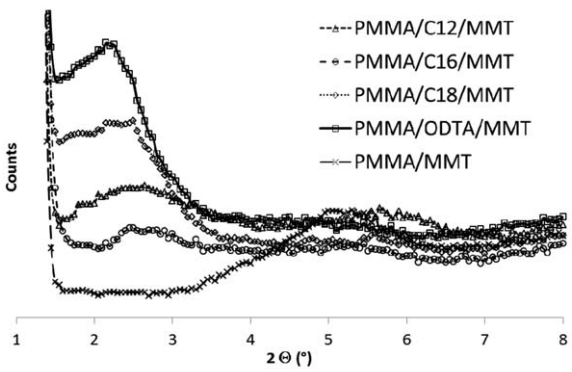

Figure 2. XRD patterns of PMMA/C_{12}/MMT, PMMA/C_{16}/MMT, PMMA/C_{18}/MMT, PMMA/ODTA/MMT, and PMMA/MMT.

In order to know the state of the clay after the modification, the amount of the various surfactants present in the modified clays was determined by TGA and elemental analyses. TGA and DTGA (in static air atmosphere) of organically modified clays are showed in Figure 1(B,C), respectively. The amount of surfactants was determined from TGA following what reported in literature,[36] and the values were compared with the ones obtained from the nitrogen determination done by elemental analysis. The results of both determinations were in good agreement and showed in the modified clays the following concentrations of surfactants: 91, 64, 58, 63 meq/100g clay in ODTA, C_{12}, C_{16}, and C_{18}/MMT, respectively.

The prepared PMMA/o-MMT contained 3 wt % of C_{12}/MMT (PMMA/C_{12}/MMT), 3 wt % of C_{16}/MMT (PMMA/C_{16}/MMT), and 3 wt % of C_{18}/MMT (PMMA/C_{18}/MMT) respect to PMMA weight. Moreover, as terms of comparison, we prepared a PMMA nanocomposite (PMMA/ODTA/MMT) using 3% of the MMT modified with a standard alkylammonium salt (ODTA) and a microcomposite obtained polymerizing MMA in the presence of 3% of pristine MMT (PMMA/MMT). XRD patterns of the nanocomposites are showed in Figure 2 and their interlayer spacings are listed in Table I.

The shift of the diffraction peak from the d° value of 1.88 nm for the C_{18}/MMT to the d value of 4.10 nm for the corresponding nanocomposite indicates that the PMMA chains are intercalated among the layers of silicate. The PMMA/C_{12}/MMT and PMMA/C_{16}/MMT present diffraction peaks corresponding to 3.68 nm and 3.18 nm, respectively, that are higher than the ones observed by C_{12}/MMT and C_{16}/MMT (1.61 nm and 1.80 nm, respectively). It is important to note that the imidazolium surfactants used to modify the MMT (C_{12}, C_{16}, and C_{18}) present in their structure a vinyl group and it is expected that

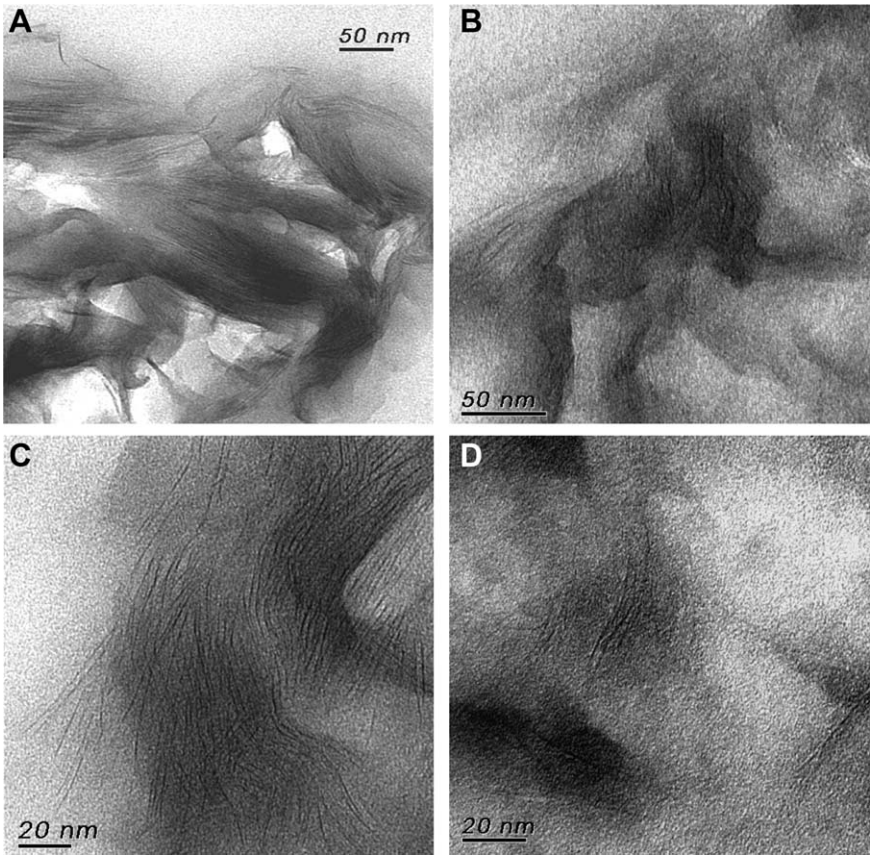

Figure 3. TEM microphotographs of PMMA/C_{12}/MMT.

some polymerization will occur on this cations, while ODTA will not be able to react by this way. In fact, by observing the Figure 2, it could be noted that the nanocomposites containing the vinyl imidazolium cations show weaker and broader peaks as compared with the one showed by the ODTA containing sample. This result suggests that the vinyl containing clays may lead, in the formation of PMMA nanocomposites, to some mixed intercalated/exfoliated structure.[14,15]

TEM

TEM was used to examine the phase morphology of nanocomposites. TEM micrographs of the ultra thin-section of PMMA/C_{12}/MMT are displayed in Figure 3. In the micrographs, the parallel dark lines represent the intersection of the MMT layers, while the gray part represents the PMMA matrix. The images show that lamellar nanocomposite has a non-uniform morphology with a heterogeneous distribution of silicate layers in the PMMA matrix. Some large tactoids dispersed in the polymer matrix can be identified [Figure 3(A)−18,000×]. Moreover, the high-magnification image [Figure 3(B)−30,000×] of the nanocomposite shows stacks containing parallel oriented layers with various degree of intercalation. On the contrary, the Figure 3(C) (48,000×) shows individual silicate layers along with two, three, and four layer stacks, which are exfoliating in the PMMA. In fact, in these area, the individual silicate sheets are separated by mean distance d of 6 nm. This value indicates a ratio between d and d° of 3.7 that being more than 3 confirms the existence of exfoliated zones.[14]

In addition, in the high-magnification micrographs [Figure 3(D) 60,000×] is possible to observe that the original aggregates of the primary particles are disrupted and individual untidy silicate layers are distributed in the polymer matrix generating an exfoliating area. Concluding, we can affirm that the PMMA/C_{12}/MMT has mixed intercalated/exfoliated nanomorphology.

Various TEM images of the PMMA/C_{18}/MMT are shown in Figure 4. Also in this case, the sample has an unhomogeneous nanomorphology. The figures show both a larger view, [Figure 4(A)−18,000X] in which is possible to note tactoids dispersed in the polymer matrix and higher magnifications that allow the individuation of discrete clay layers [Figure 4(B)−24,000×, Figure 4(C)−36,000×, and Figure 4(D)−60,000×]. These images show that also the PMMA/C_{18}/MMT structure appears to be mixed intercalated/delaminated.

In any case, at the end of this section, a word of caution has to be spent on the information obtained. XRD and TEM are effective tools, but they are limited in that they only probe a small volume of the sample. Then from these analyses, it is difficult to draw conclusions on the degree of intercalation, exfoliation, and dispersion. We have already shown[7,37] that TGA study of kinetic parameters of degradation process is an effective method to obtain information on the degree of exfoliation and then we carried out this kind of study, following the procedure described in those papers, whose results are discussed at the end of next section.

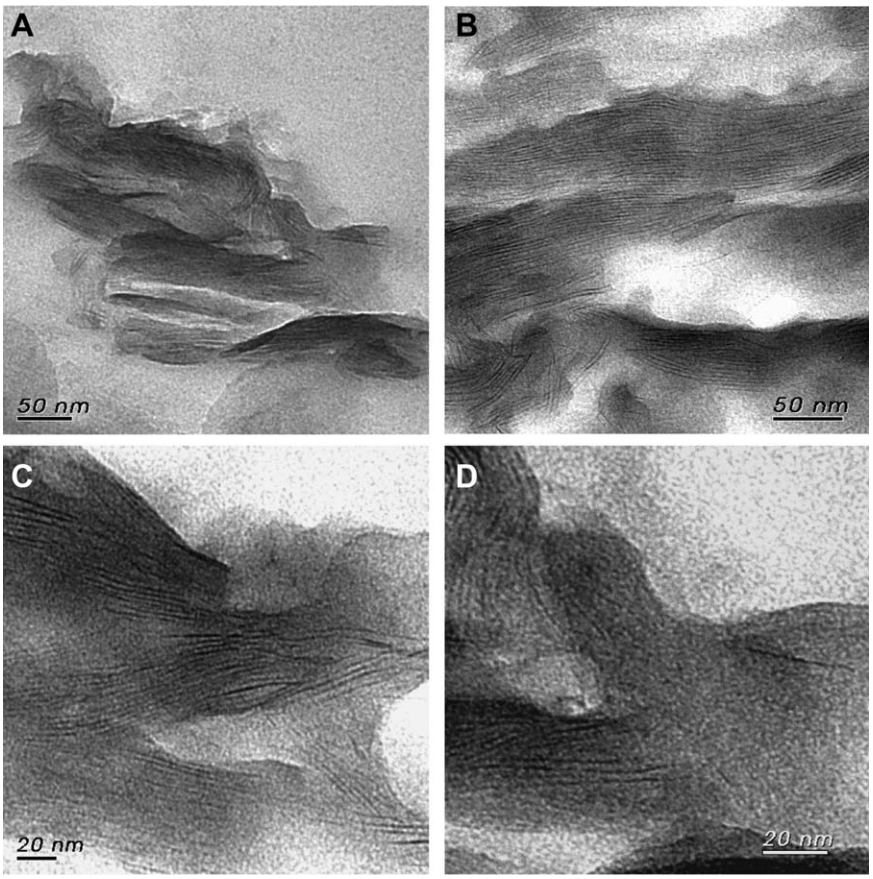

Figure 4. TEM microphotographs of PMMA/C_{18}/MMT.

Thermal Degradation

In bulk processing of nanocomposites, elevated temperatures are usually required, so the thermal stability of the organic surfactants used to modify the MMT plays a fundamental role. It is well known that the commonly used ammonium cationic surfactants undergo Hoffman thermal degradation in the temperature range of 150–300°C and present poor thermal stability. To solve this problem, we prepared MMTs organically modified with thermally stable imidazolium surfactant and we compared their thermal stability (studied by TGA) with the one of the o-MMT obtained using a conventional ammonium cationic surfactant (ODTA/MMT). Considering the temperature of decomposition as the temperature at which the residue percentage reaches 90% (T_{d10}) with respect to the initial weight, the results show an increase of T_{d10} in nitrogen of 292°C, 229°C, and 202°C (for C_{12}, C_{16}, and C_{18} /MMTs, respectively) as compared with ODTA containing MMT (Table I).

The o-MMTs were used to prepare a series of PMMA nanocomposites. The thermal stability of nanocomposites was studied by TGA (Table I). The TGA and DTGA curves are displayed in Figure 5. First, the results show an increase of T_{d10} (18°C) in the PMMA/ODTA/MMT sample as compared with pure PMMA and with PMMA/MMT microcomposite. This is obviously due to the formation of an intercalated nanocomposite in the former case and is in agreement with what is reported in literature. In fact, in PMMA/o-MMT nanocomposites the intercalation of PMMA chains between the silicate layers is enhanced by the strong polar interaction developed between the oxygen groups of the silicate and the oxygen groups of PMMA.[38,39] Moreover, it is reported[35] that the enhanced thermal stability of PMMA intercalated within the clay is due to both the difference of chemical structure and restricted thermal motion of polymer chains in the silicate interlayer. On the contrary, in conventional composites obtained using pristine MMT, the PMMA chains cannot enter in the narrow interlayer of hydrophilic silicate and consequently the strong interactions, present in nanocomposite, are absent.

Comparing the decomposition temperatures in nitrogen of PMMA/C_{18}/MMT and PMMA/ODTA/MMT, we observed an increase of the T_{d10} of 27°C for the nanocomposite containing the imidazolium surfactant. This result could be due to a higher polymer molecular weight in the PMMA/C_{18}/MMT and/or to a better surfactant thermal stability and/or a higher degree of exfoliation. Because, from the GPC measurements, the PMMA M_ws in the two nanocomposites are similar (50.69×10^4 and 54.16×10^4, respectively, Table I), we can conclude that the higher thermal stability of the delocalized imidazolium cation (Table I) and a higher degree of exfoliation confer an improvement of thermal properties to imidazolium cation-containing nanocomposite. The T_{d10} values of PMMA/C_{12}/MMT (291°C), PMMA/C_{16}/MMT (291°C), and PMMA/ODTA/MMT (292°C) can be explained taking into account two contributions: difference in M_ws and nanomorphology. The PMMA M_ws in PMMA/C_{12}/MMT and PMMA/C_{16}/MMT (33.38×10^{-4} and

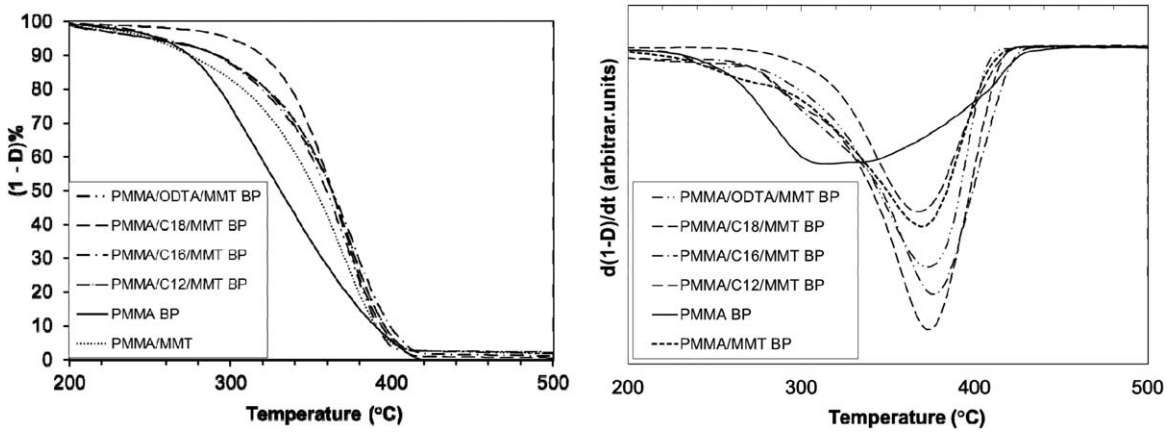

Figure 5. TGA and DTGA curves under flowing nitrogen of PMMA/ODTA/MMT BP, PMMA/C_{18}/MMT BP, PMMA/C_{16}/MMT BP, PMMAC_{12}/MMT BP, PMMA BP, and PMMA/MMT BP.

39.50×10^{-4}, respectively) are lower than the PMMA/ODTA/MMT M_w (Table I). This trend, due to the predominant M_w influence on thermal stability of PMMA nanocomposites, can be used to rationalize the small differences among the T_{d10} values of samples reported in Table I. Moreover, these results can be explained in terms of similar nanomorphologies of the samples. In this case, the achievement of the same degree of exfoliation can be explained considering that, during the polymerization reaction, the molecules of MMA are able to more easily enter inside ODTA/MMT galleries (2.05 nm) that in those of C_{12}/MMT (1.61 nm) and C_{16}/MMT (1.80).

To confirm this hypothesis, we determined, in nitrogen atmosphere, the apparent activation energy (E_a) of the degradation process of some of our samples. As already mentioned, we have shown[7,37] that the comparison of the E_a values of samples having the same matrix is an useful, relatively cheap tool to draw conclusion on the state of the clay nanodispersion. The results of the E_a determination are reported in Table II.

The trend showed by the E_a values confirms that PMMA/C_{18}/MMT obtained by bulk polymerization (BP) sample has the higher degree of exfoliation that determines an increase of the apparent activation energy (188 kJ mol^{-1}), about 20% higher than pure PMMA BP (156 kJ mol^{-1}). The other BP samples have E_a values higher than PMMA and close to each other (in the range 166–169 kJ mol^{-1}) as the result of a lower degree of exfoliation.

As a further confirmation of thermal property dependence from nanomorphology these last samples have undergone a process of solution blending (SB). Comparing sample PMMA/ODTA/MMT SB to PMMA/ODTA/MMT BP, the thermogravimetric data (reported in Table I and Figure 6) show an increase in the value of T_{d5} and T_{d10} of 30 and 15°C, respectively. Furthermore, by comparing the decomposition temperatures in nitrogen of PMMA/C_{12}/MMT BP and PMMA/C_{16}/MMT BP with corresponding samples obtained from SB is observed an increase of the values of T_{d5} (of 42 and 41°C, respectively) and T_{d10} (of 17°C and 21°C, respectively). Figure 6 shows the TGA curves of some nanocomposites prepared by BP and SB.

Comparing the E_a values of BP and SB samples, it is evident that SB samples exhibit a better thermal stability because of their higher degree of exfoliation compared to BP samples. In fact, while PMMA/C_{18}/MMT SB shows a slightly increase of E_a with respect to PMMA/C_{18}/MMT BP (from 188 to 195 kJ mol^{-1}), the other SB samples show a more marked enhancement (e.g., in the case of PMMA/C_{16}/MMT from 167 to 188 kJ mol^{-1}). It is likely that the solvent molecules entering within the galleries of the o-MMT facilitate the polymer chain insertion between the layers of the phyllosilicate, and, therefore, the exfoliation process.

DMA and Nanoindentation Measurements

The nanomorphology influences mechanical performance also. To confirm this, we carried out on some of our samples DMA measurements to determine elastic storage modulus and T_g (through the tan δ maximum) and nanoindentation measurements to determine elastic modulus and hardness.

It is important to take into account that the results of DMA and nanoindentation measurements often do not agree well with those obtained from mechanical testing methods.[40] In most cases, the elastic storage modulus measured by DMA is utilized only for screening the material properties for the purposes of quality control, research and development of optimum processing conditions. However, the values relative to a native PMMA are in good agreement with those reported in the literature (Young's modulus 1.8–3.1 GPa).[41]

The obtained data (Figure 7 and Table III) show that the measured properties are influenced by the degree of dispersion of the nanoplatelet into the PMMA matrix. In fact, among the BP samples, the higher values of elastic modulus have been obtained for the PMMA/C_{18}/MMT BP (2.47 GPa from DMA and 4.09 from nanoindentation) while for pure PMMA the values are 1.87 and 1.83 GPa, respectively. Beside to the elastic modulus increase, an significant enhancement of hardness has been detected (from 0.48 GPa for PMMA to 1.57 GPa) in PMMA/C_{18}/MMT BP. The microcomposite PMMA/MMT BP shows the lower increase of the measured properties, while the other nanocomposites, which have a similar nanodispersion degree of the MMT layers, show modulus and hardness very close. Concerning T_g's, while the microcomposite has a T_g (127°C) slightly lower that PMMA (129°C), all the other BP samples show a higher Tg, in the range 131–138°C, in some way proportional to exfoliation degree.

Table II. Apparent Activation Energy (E_a) of Pure PMMA, BP, and SB Nanocomposite

	T_{max} (°C)[a] at the given heating rate (°C min^{-1})								
Sample	2	5	7.5	10	12.5	15	17.5	20	E_a (kJ mol^{-1})[a]
PMMA BP	288	304	310	315	319	322	325	327	156
PMMA/MMT/ODTA BP	345	358	365	372	378	382	385	387	166
PMMA/C_{12}/MMT BP	340	357	367	372	375	378	380	382	169
PMMA/C_{16}/MMT BP	343	359	365	375	378	381	383	385	167
PMMA/C_{18}/MMT BP	346	359	365	372	376	379	384	386	188
PMMA/MMT/ODTA SB	346	359	366	373	377	381	383	385	182
PMMA/C_{12}/MMT SB	345	358	366	371	374	379	381	384	187
PMMA/C_{16}/MMT SB	347	360	367	374	377	380	383	386	188
PMMA/C_{18}/MMT SB	348	360	367	373	375	379	383	386	195

[a] Determined in nitrogen.

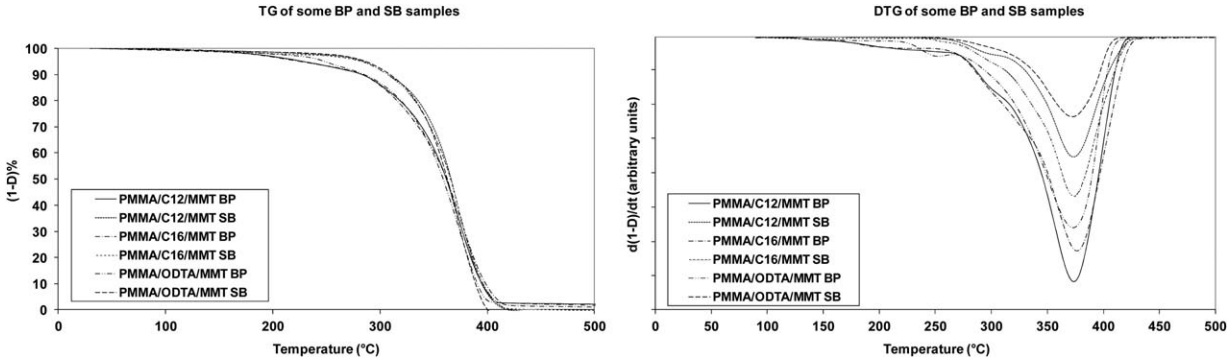

Figure 6. TGA and DTGA curves under flowing nitrogen of PMMA/ODTA/MMT BP, PMMA/C_{16}/MMT BP, PMMA/C_{12}/MMT BP, PMMA/ODTA/MMT SB, PMMA/C_{16}/MMT SB, and PMMA/C_{12}/MMT3 SB.

The SB treatment, promoting a solvent driven exfoliation, would have produced a further improvement of properties, and this is what we observed. In fact, all the detected values of elastic modulus, hardness and T_g for the SB samples are higher than BP ones, with the PMMA/C_{18}/MMT SB showing again the higher values (Table III).

CONCLUSIONS

In conclusion, among the nanocomposites obtained by BP higher thermal stability and better mechanical properties were recorded

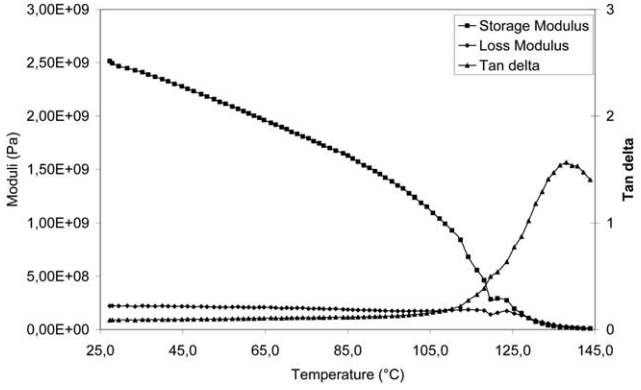

Figure 7. Storage modulus, loss modulus, and tan δ as a function of temperature for sample PMMA/C_{18}/MMT BP.

Table III. Elastic Storage Modulus and T_g (Determined by DMA), Elastic Modulus and Hardness (Determined by Nanoindentation) of BP and SB Nanocomposites at 30°C

Sample	Elastic storage modulus (GPa)[a]	T_g (°C)[a]	Elastic modulus (GPa)[b]	Hardness (GPa)[b]
PMMA	1.87	129	1.83	0.48
PMMA/MMT BP	2.05	127	3.14	1.15
PMMA/ODTA/MMT BP	2.17	134	3.45	1.22
PMMA/C_{12}/MMT BP	2.12	131	3.41	1.20
PMMA/C_{16}/MMT BP	2.15	134	3.48	1.25
PMMA/C_{18}/MMT BP	2.47	138	4.09	1.57
PMMA/ODTA/MMT SB	2.45	144	3.65	1.45
PMMA/C_{12}/MMT SB	2.33	143	3.29	1.43
PMMA/C_{16}/MMT SB	2.47	144	3.90	1.40
PMMA/C_{18}/MMT SB	3.09	146	4.48	1.83

[a] Data determined by DMA measurements.
[b] Data determined by nanoindentation measurements.

in the PMMA/C_{18}/MMT BP sample, while the nanocomposites prepared from modified clays with the cations C_{12}, C_{16}, and ODTA show similar performances among them. These results are attributed to a higher degree of exfoliation in the sample PMMA/C_{18}/MMT BP. Unfortunately from XRD and TEM, data were not possible to obtain definitive and quantitative information on the degree of exfoliation, but kinetics study of the degradation process (through the E_a determination) confirms the influence of degree of exfoliation on thermal stability. Moreover, the fact that all of the nanocomposites obtained from SB exhibit thermal degradation temperatures higher than the corresponding samples obtained via BP, and very close to PMMA/C_{18}/MMT BP, further supports the hypothesis that exfoliation degree is the main factor determining the best thermal properties. The greater thermal stability of exfoliated nanocomposites compared to microcomposites or nanocomposites with intercalated structure is due to a barrier effect played by the layers of the phyllosilicates. In the SB process solvent molecules, due to the nature of the organophilic surfactants, are able to penetrate within the galleries of the o-MMT favoring the separations between the layers and, consequently, the formation of exfoliated structures. The consequent enhancement of the nanofiller dispersion produces a further increase in nanocomposite performances.

REFERENCES

1. Gopakumar, T. G.; Lee, J. A.; Kontopoulou, M.; Parent, J. S. *Polymer* **2002**, *43*, 5483.
2. Santamaría, P.; Eguiazabal, J. I. *Polym. Adv. Technol.* **2013**, *24*, 300.
3. Ludueña, L. N.; Vázquez, A.; Alvarez, V. A. *J. Appl. Polym. Sci.* **2013**, *128*, 2648.
4. Soulestin, J.; Rashmi, B. J.; Bourbigot, S.; Lacrampe, M. F.; Krawczak, P. *Macromol. Mater. Eng.* **2012**, *297*, 444.
5. Moraes, R. P.; Valera, T. S.; Pereira, A. M. C.; Demarquette, N. R.; Santos, A. M. *J. Appl. Polym. Sci.* **2011**, *119*, 3658.
6. Pack, S.; Kashiwagi, T.; Cao, C.; Korach, C. S.; Lewin, M.; Rafailovich, M. H. *Macromolecules* **2010**, *43*, 5338.
7. Bottino, F. A.; Di Pasquale, G.; Fabbri, E.; Orestano, A.; Pollicino, A. *Polym. Degrad. Stab.* **2009**, *94*, 369.
8. Vaia, R. A.; Giannelis, E. P. *Macromolecules* **1997**, *30*, 7990.
9. Vaia, R. A.; Giannelis, E. P. *Macromolecules* **1997**, *30*, 8000.
10. Pandey, J. K.; Raghunatha Reddy, K.; Pratheep Kumar, A.; Singh, R. P. *Polym. Degrad. Stab.* **2005**, *88*, 234.
11. Gilman, J. W.; Awad, W. H.; Davis, R. D., Shields, J.; Harris, R. H., Jr.; Davis, C.; Morgan, A. B.; Sutto, T. E.; Callahan, J.; Trulove, P. C.; DeLong, H. C. *Chem. Mater.* **2002**, *14*, 3776.
12. Wang, Z. M.; Chung, T. C.; Gilman, J. W.; Manias, E. *J. Polym. Sci. Part B: Polym. Phys.* **2003**, *41*, 3173.
13. Bottino, F. A.; Fabbri, E.; Fragalà, I. L.; Malandrino, G.; Orestano, A.; Pilati, F.; Pollicino, A. *Macromol. Rapid Commun.* **2003**, *24*, 1079.
14. Awada, W. H.; Gilman, J. W.; Nyden, M.; Harris, R. H., Jr.; Sutto, T. E.; Callahan, J.; Trulove, P. C.; DeLong, H. C.; Fox, D. M. *Thermochim. Acta* **2004**, *409*, 3.
15. Zhao, J.; Morgan, A. B.; Harris, J. D. *Polymer* **2005**, *46*, 8641.
16. Kim, N. H.; Malhotra, S. V.; Xanthos, M. *Microporous Mesoporous Mater.* **2006**, *96*, 29.
17. Modesti, M.; Besco, S.; Lorenzetti, A.; Causin, V.; Marega, C.; Gilman, J. W.; Fox, D. M.; Trulove, P. C.; De Long, H. C.; Zammarano, M. *Polym. Degrad. Stab.* **2007**, *92*, 2206.
18. Stoeffler, K.; Lafleur, P. G.; Denault, J. *Polym. Degrad. Stab.* **2008**, *93*, 1332.
19. Cui, L.; Bara, J. E.; Brun, Y.; Yoo, Y.; Yoon, P. J.; Paul, D. R. *Polymer* **2009**, *50*, 2492.
20. Livi, S; Duchet-Rumeau, J.; Pham, T. N.; Gérard, J. F. *J. Colloid Interface Sci.* **2010**, *349*, 424.
21. Livi, S; Duchet-Rumeau, J.; Pham, T. N.; Gérard, J. F. *J. Colloid Interface Sci.* **2011**, *354*, 555.
22. Xu, H.; Tong, F.; Yu, J.; Wen, L.; Zhang, J.; He, J. *Polym. Int.* **2012**, *61*, 1382.
23. Zhang, R. C.; Hong, S. M.; Koo, C. M. *J. Appl. Polym. Sci.* **2014**, *131*, 40648.
24. Lee, D. C.; Jang, L. W. *J. Appl. Polym. Sci.* **1996**, *61*, 1117.
25. Zeng, C. C.; Lee, L. *J. Macromolecules* **2001**, *34*, 4098.
26. Kumar, S.; Jog, J. P.; Natarajan, U. *J. Appl. Polym. Sci.* **2003**, *89*, 1186.
27. Jash, P.; Wilkie, C. A. *Polym. Degrad. Stab.* **2005**, *88*, 401.
28. Dhibar, A. K.; Mallick, S.; Rath, T.; Khatua, B. B. *J. Appl. Polym. Sci.* **2009**, *113*, 3012.
29. Mohanty, S.; Nayak, S. K. *J. Thermoplast. Compos. Mater.* **2010**, *23*, 623.
30. Unnikrishnan, L.; Mohanty, S.; Nayak, S. K.; Ali, A. *Mater. Sci. Eng. A* **2011**, *528*, 3943.
31. Yamagata, S.; Hamba, Y.; Akasaka, T.; Ushijima, N.; Uo, M.; Iida, J.; Watari, F. *Appl. Surf. Sci.* **2012**, *262*, 56.
32. Tsai, T.-Y.; Lin, M.-J.; Chuang, Y.-C.; Chou, P.-C. *Mater. Chem. Phys.* **2013**, *138*, 230.
33. Valandro, S. R.; Lombardo, P. C.; Poli, A. L.; Horn, M. A, Jr.; Neumann, M. G.; Cavalheiro, C. C. S. *Mater. Res.* **2014**, *17*, 265.
34. Vaia, R. A. In Polymer Clay Nanocomposites; Pinnavaia, T. J.; Beall, G. W., Eds.; Wiley: London, **2000**; pp 229–266.
35. Zhu, J.; Start, P.; Mauritz, K. A.; Wilkie, C. A.; *Polym. Degrad. Stab.* **2002**, *77*, 253.
36. Vazquez, A.; Lopez, M.; Kortaberria, G.; Martin, L.; Mondragon, I. *Appl. Clay Sci.* **2008**, *41*, 24.
37. Abate, L.; Blanco, I.; Bottino, F. A.; Di Pasquale, G.; Fabbri, E.; Orestano, A.; Pollicino, A. *J. Therm. Anal. Calorim.* **2008**, *91*, 681.
38. Okamoto, M.; Morita, S.; Kim, Y. H.; Kotaka, T.; Tateyama, H. *Polymer* **2000**, *41*, 3887.
39. Moussaif, N.; Groeninckx, G. *Polymer* **2003**, *44*, 7899.
40. Lee-Sullivan, P.; Dykeman, D. *Polym. Test.* **2000**, *19*, 155.
41. Brandrup, J.; Immergut, E. H., Eds. Polymer Handbook, 3rd ed.; Wiley, 1989; Livermore, C.; Voldman, J. "MIT Material Property Database".